SMYD3: a new regulator of the early steps of adipocyte differentiation

Federica Gilardi (federica.gilardi@chuv.ch)
Lausanne University Hospital https://orcid.org/0000-0001-5421-2779
Tatjana Sajic
Marie Gasser
Tiziana Caputo
Harvard Medical School
Nasim Bararpour
Marc Augsburger
https://orcid.org/0000-0002-5606-3831
Nadia Walter
Alexander Hainard
Tony Fracasso
Aurelien Thomas

Article

Keywords:

Posted Date: July 6th, 2023

DOI: https://doi.org/10.21203/rs.3.rs-3126142/v1

Additional Declarations: There is **NO** conflict of interest to disclose

SMYD3: a new regulator of the early steps of adipocyte differentiation

Tatjana Sajic[1,2], Marie Gasser[1,2], Tiziana Caputo[3], Nasim Bararpour[4,5], Marc Augsburger[1], Nadia Walter[6], Alexandre Hainard[6], Tony Fracasso[7], Aurélien Thomas[1,2], Federica Gilardi[1,2]

1. Unit of Forensic Toxicology and Chemistry, CURML, Lausanne and Geneva University Hospitals, Lausanne, Geneva, Switzerland.

2. Faculty Unit of Toxicology, CURML, Faculty of Biology and Medicine, University of Lausanne, Lausanne, Switzerland.

3. Section on Integrative Physiology and Metabolism, Joslin Diabetes Center, Harvard Medical School, Boston, MA, USA

4. Stanford Center for Genomics and Personalized Medicine, Stanford, CA, USA

5. Department of Genetics, Stanford University, Stanford, CA, USA

6. Proteomics Core Facility, Faculty of Medicine, University of Geneva, Geneva, Switzerland

7. Unit of Forensic Medicine, CURML, Lausanne and Geneva University Hospitals, Lausanne, Geneva, Switzerland

Corresponding author:

Federica Gilardi PhD

Faculty Unit of Toxicology

Chemin de la Vulliette 4

1000 Lausanne 25

Switzerland

Phone number: +41 22 379 55 78

Email: federica.gilardi@chuv.ch

Abstract

Background

In obesity, adipose tissue undergoes a remodeling process characterized by increased adipocyte size (hypertrophia) and number (hyperplasia). The individual ability to tip the balance toward the hyperplastic growth, with recruitment of new fat cells through adipogenesis, seems to be critical for a healthy adipose tissue expansion, as opposed to the development of inflammation and detrimental metabolic consequences. However, the molecular mechanisms underlying this fine-tuned regulation are far from being understood.

Methods

We analyzed by mass spectrometry-based proteomics visceral white adipose tissue (vWAT) samples collected from C57BL6 mice fed with a HFD for 8 weeks. A subset of these mice, called low inflammation (Low-INFL), showed a low susceptibility to the onset of adipose tissue inflammation, as opposed to those developing the expected inflammatory response (Hi-INFL). We identified the discriminants between Low-INFL and Hi-INFL vWAT samples and explored their function in Adipose Derived human Mesenchymal Stem Cells (AD-hMSCs) differentiated to adipocytes.

Results

We quantified 6051 proteins. Among the candidates that most differentiate Low-INFL from Hi-INFL vWAT, we found proteins involved in adipocyte function, including adiponectin and hormone sensitive lipase, suggesting that adipocyte differentiation is enhanced in Low-INFL, as compared to Hi-INFL. The chromatin modifier SET and MYND Domain Containing 3 (SMYD3), whose function in adipose tissue was so far unknown, was another top-scored hit. SMYD3 expression was significantly higher in Low-INFL vWAT, as confirmed by western blot analysis. *In vitro*, we found that SMYD3 mRNA and protein levels decrease rapidly along the differentiation process of AD-hMSCs. Moreover, SMYD3 knock-down at the beginning of adipocyte differentiation resulted in reduced cell proliferation and, at longer term, reduced lipid accumulation in adipocytes.

Conclusions

Our study describes an important role of SMYD3 as a newly discovered regulator of adipocyte proliferation during the early steps of adipogenesis.

Introduction

The etiology of obesity is multifactorial and involves an interaction between genetic and environmental factors (1). Obesity is driven by the unbalance between calorie intake and consumption, which results in the abnormal accumulation of white adipose tissue (WAT). WAT expansion occurs through both hyperplasia, by favoring the differentiation of adipocyte precursors to increase the number of adipocytes, and hypertrophy, by enlarging the size of existing adipocytes (2). In addition, a huge remodeling of the cellular composition of the tissue takes place, with recruitment of pro-inflammatory immune cells. The activation of this local inflammatory response is considered as the key event in the development of the detrimental consequences of obesity, such as metabolic syndrome (3). Interestingly, however, many obese individuals are relatively resistant to developing these complications (4-6), which raises questions about possible factors modulating the susceptibility to obesity-driven inflammation and metabolic consequences(7).

In the last years, converging reports have suggested that the ability to recruit new fat cells through adipogenesis, which would favor the hyperplastic over the hypertrophic expansion of the tissue, is a critical determinant of a healthy adipose tissue remodeling with reduced activation of pro-inflammatory pathways in obesity(7). During adipogenesis, mesenchymal precursors first commit themselves to the adipocyte lineage. This step is followed by terminal differentiation, where committed pre-adipocytes acquire the characteristics of mature adipocytes. The regulation of this differentiation process has been extensively studied over the past three decades using, in particular, several fibroblast-like cell culture models that differentiate to adipocytes in response to a hormonal cocktail (reviewed in (8)). However, which molecular players would favor adipogenesis to drive a healthy tissue expansion *in vivo*, and how, is far from being understood. Among others, epigenetic mechanisms, which can alter gene transcription in response to environmental inputs, seem very good candidates as fine-tuning regulators of the individual vulnerability to obesity-driven detrimental consequences.

Epigenetics refers to chemical modifications, including acetylation, methylation, phosphorylation, ubiquitination etc., of either single nucleotides and/or histones that occur without a change in the DNA sequence. These changes can profoundly affect gene transcription and protein expression as well as

DNA replication(9). Several groups reported effects of epigenetic regulators on adipogenesis. For example, class I Histone deacetylases (HDACs), particularly HDAC3, has emerged as important regulators of the differentiation of adipocytes and drivers of the metabolic features of these cells toward a brown phenotype (10-12). The histone methyltransferase G9a promotes the di-methylation of the histone H3K9 in the promoter of PPARγ gene, thereby blocking its transcription and subsequently adipocyte differentiation (13). Also, the histone methyltransferase SETDB1 mediates H3K9 trimethylation on PPARγ and CEBPα genes, thus keeping their expression low and allowing adipocytes to remain primed for differentiation (14), while the histone lysine demethylase 1 (LSD1) promotes adipocyte differentiation by decreasing H3K9 dimethylation at the CEBPα promoter(15).

Here, we took advantage of a sub-set of visceral white adipose tissue (vWAT) samples collected from C57BL6 mice fed with a HFD for 8 weeks, that we called low inflammation (Low-INFL), showing a low susceptibility to the onset of adipose tissue inflammation, as opposed to their high inflammation (Hi-INFL) counterpart. We applied Data-Independent Acquisition Mass Spectrometry (DIA-MS) based proteomic analysis on vWAT samples from Low-INFL and Hi-INFL mice and quantified more than 6000 proteins. We experimentally validated our results by orthogonal analytical approaches and functional *in-vitro* experiments that allowed us to highlight the chromatin modifier SET And MYND Domain Containing 3 (SMYD3) as a new regulator of adipocyte proliferation, participating to the early steps of adipogenesis.

Material and Methods

Animal experiments

All animal experiments were approved by the Swiss Veterinary Office (VD-2942.b) and were previously described (16). In brief, C57/BL6 male mice were from Janvier Labs and housed 5 per cage. Four-week-old mice were fed for 2 weeks with a 10% in fat chow diet (D12450J, Research Diet). At 6 weeks mice were either shifted to a high-fat diet (HFD) containing 60% fat (D12492, Research Diet or kept on a control diet for 8 weeks (n=60). Random blocking was used. All animals were kept in a 12:12 h light:dark cycle with water and food ad libitum. All the mice were killed by CO2 between ZT2 and ZT5.

The onset of visceral adipose tissue inflammation after 8 weeks of HFD was assessed by measurement of the following parameters: circulating levels of insulin, resistin and leptin levels, and expression of *Cxcl212*, *Ccl2* and *Itgax* in vWAT in all HFD mice as compared to 20 randomly picked control mice. All these measurements, in addition to the individual mouse weight, were used as variables to perform a Principal Component Analysis (PCA) and HFD-fed mice were classified as Low Inflammation (Low-INFL) when they were clustering close to the control group, as opposed to the High Inflammation (Hi-INFL) mice (16).

Plasma Biochemistry

Circulating levels of insulin, resistin and leptin were simultaneously measured in plasma samples using a ProcartaPlex Multiplex Immunoassay (Life Technologies Europe, Switzerland), on a Luminex 200 system, according to the manufacturers' instructions.

Proteomics analysis of vWAT by data-independent acquisition mass spectrometry (DIA-MS)

Proteomic analysis was performed starting from 30mg of snap-frozen visceral adipose tissue per mice. Samples were homogenized in 500µl of ice-cold phosphate-buffered saline (PBS, #10010015, Gibco) and the soluble tissue proteins were precipitated with trichloroacetic acid (TCA) and washed with ice-cold acetone.

Purified protein pellets were dissolved in 8 M urea buffer and digested overnight with a ratio of 1µg trypsin (#V5113, Promega) for 20µg protein. Generated peptide digests were cleaned on MACROSpin Plate-Vydac Silica C18 (Nest Group Inc., Southborough, MA), solubilized in 30µL of 0.1% aqueous formic acid (FA) with 2% acetonitrile (ACN). Indexed retention time (iRT) peptides were added (RT-kit WR, Biognosys) in equal 1 pmol/µL amount into each sample prior to mass spectrometry (MS) injection. Peptides digests of respective samples were processed by liquid chromatography-electrospray ionization tandem mass spectrometry (LC-ESI-MS/MS) on an Orbitrap Fusion Lumos Tribrid mass spectrometer (Thermo Fisher Scientific) equipped with an Easy nLC1200 liquid chromatography system (Thermo Fisher Scientific). Raw data analysis, generation of peptide and protein matrices were performed with commercial proteomic software Spectronaut (version:14.8.201029.47784, Biognosys, https://biognosys.com/software/spectronaut/) as described previously(17, 18). The successive steps of LC-MS analysis and raw data processing are detailed in Supplementary material.

Statistical analysis and visualization of vWAT proteomics data

R software for statistical computing and graphics (version:3.6.1) was used for data analysis and visualization. To explore the changes induced by HFD in Low-INFL and Hi-INFL groups, we performed Limma analysis (19) on generated protein matrix. Two-sided p-values were adjusted for the number of tests performed via a Benjamini-Hochberg (BH) FDR-based correction (adj.p) and proteins with adj.p.<0.05 and fold change (FC) ≥ 1.5 were considered as differentially expressed.

To independently select the most descriptive features for each tissue group from large protein data matrix (6051 protein), we used Supervised Partial Least Squares Discriminant Analysis (PLS-DA) trough mixOmics' R package (version 6.10.9) and imputed 3 components with limited number of features per component (N=100).

GO Enrichment analysis was performed using R package Disease Ontology (DO) Semantic and Enrichment (DOSE, version 3.14.3) (20). As input lists, we used differential proteins from each respective comparison. UniProt IDs were converted to GeneIDs and enrichment analysis was

performed for biological process or "BP" subontology against mouse genome database "org.Mm.eg.db." and under FDR control set up to 0.05. We reported all enrichment GO categories with FDR <0.05 and with minimum 3 and maximum 50 genes annotated by Ontology term.

Cell culture and treatment

Adipose-derived human Mesenchymal Stem Cells (AD-hMSCs, Lifeline Cell Technology, Frederick, MD, USA) were expanded at 37°C and 5% CO2 in Mesenchimal Stem Cell Growth Medium 2, supplemented with Mesenchymal Stem Cell Growth Medium 2 Supplement Mix (PromoCell, Heidelberg, Germany). For differentiation experiments, confluent cells were switched to Mesenchymal Stem Cell Growth Medium 2 supplemented 10% Foetal Bovine Serum (Biowest #S1810-500, Nuaillé, France), 0.2µM Indomethacine (Sigma-Aldrich, #I7378), 10µg/ml insulin (Sigma-Aldrich #I2643), 1µM dexamethasone (Sigma-Aldrich #D2915), and 0.5mM Isobutylmethylxanthine (Sigma-Aldrich, #I7018), to induce the differentiation into adipocytes. Medium was replenished every three days. For cell growth measurements, cells were detached with TrypLE Express (Gibco, #12304-021, Thermofisher) and were counted with a Cell Countess II FL (Thermofisher Scientific).

RNA silencing

AD-hMSCs at 70% of confluence were detached with TrypLE (Gibco), transfected with 20nM of hSMYD3 Silencer Select pre-designed siRNAs (Ambion, clone s34865, ThermoFisher) or Silencer™ Negative Control (Ambion #AM4611) using Lipofectamine RNAiMAX Reagent (Invitrogen, #13778. Thermofisher), following manufacturer's instructions, and plated. After 48h, undifferentiated cells were harvested, or differentiation was induced as described above.

Proliferation assay

Cell proliferation was assessed using the Cell Proliferation Kit I (MTT) (Roche Diagnostics, #11465007001, Mannheim, Germany) following manufacturer instructions. The plates were incubated at 37°C and 5% CO_2 for 20 minutes with the MTT reaction mix and DMSO was used to extract the coloration. The absorbance was measured in duplicate at 540 nm with an Infinite M Nano Reader (Tecan, Männedorf, Switzerland).

Oil Red O staining

After 14 days of differentiation, cells were washed once in PBS and fixed with formaldehyde for 15 minutes. The staining solution (Sigma-Aldrich #O1391) was diluted 60:40 in distilled water, filtered after 1 hours and added to dishes for 4 hours. Excessive staining solution was removed and cells were washed twice with distilled water. After taking pictures, the lipid staining was extracted with DMSO and the absorbance was measured in duplicate at 455 nm with an Infinite M Nano Reader (Tecan, Männedorf, Switzerland).

RNA Extraction and quantitative PCR

Total RNA was isolated from undifferentiated and differentiated cells, or from adipose tissue, using the Direct-zol RNA MiniPrep Kit (ZymoResearch, #R2052, Lucerna-Chem, Luzern, Switzerland) following manufacturer protocol. cDNA was synthesized using 100 ng of total RNA with the iScript cDNA Synthesis Kit (BioRad, #1708891, Cressier, Switzerland) following manufacturer instructions. For real-time quantitative PCR, KAPA PROBE FAST qPCR Master Mix (2X) Kit or KAPA SYBR FAST qPCR Master Mix (2X) Kit were used (KapaBiosystems, #KK4703 or #KK4602, Sigma-Aldrich). The primer sets are shown in Supplementary Table 1. Ribosomal Protein S13 (RPS13) was used as a housekeeping gene and the relative expression was calculated with the $2^{-\Delta\Delta Ct}$ method.

Western blotting

Whole proteins were extracted using mPER Mammalian Protein Extraction Reagent (Thermofisher, #78501) supplemented with Halt protease inhibitor (Thermofisher, #78426) and Halt phosphatase inhibitor (Thermofisher, #78429) cocktails. For adipose tissue extracts, the lysates were left 1 h at 4 °C on a rotating wheel and then sonicated 5 cycles 30″ ON/30″ OFF, using a Bioruptor Pico (Diagenode, Liège, Belgium). Protein concentration was determined by Pierce BSA protein assay Kit (Pierce, #23227, Thermofisher). 10–15 µg of lysates was applied to SDS-PAGE. Anti-SMYD3 (Diagenode, #C15410253, used at 1:1000), anti-GAPDH (Cell signaling, #2118s, used 1:1000), anti-rabbit HRP for ECL (GE Healthcare, #NA934V, used at 1:10000) antibodies were used for western blot. Detection

was performed with ECL Select kit (Cytiva, #RPN2235, Amersham, Sigma-Aldrich) in a Syngene G:BOX. Quantification of band density was performed with ImageJ.

Statistical analysis

For proteomics studies, statistical analyses were performed in the R environment, as described above. For cell experiments data are represented as mean± SEM and statistical tests were performed using GraphPad Prism version 9.1.0 for Windows (GraphPad Software, San Diego, CA, USA, www.graphpad.com).

Results

To identify new players in the fine-tuning of WAT response to nutritional challenges (i.e. HFD), we investigated a set of vWAT samples collected from C57/BL6j male mice fed either a HFD or a chow diet for 8 weeks(16). As expected, HFD induced a strong vWAT expansion. However, and most interestingly, when we evaluated the inflammatory status of vWAT, we found that in a subgroup of mice fed with the HFD (about 30%) the development of vWAT inflammation was limited. In particular, in this subgroup of HFD-fed mice, that we named Low-INFL mice, vWAT expression of *Ccl2, Cxcl12*, and *Itgax* and the circulating levels of insulin, resistin and leptin, which are associated with vWAT inflammation, were significantly lower with respect to the other HFD-fed mice, thereafter named Hi-INFL (Figure 1A, B). In contrast, the accumulation of vWAT was comparable in both Low-INFL and Hi-INFL groups, suggesting that, in Low-INFL mice, a healthier expansion of vWAT takes place in response to the HFD (Figure 1C). We reasoned that this different susceptibility to the detrimental effects of HFD is of great interest to identify key molecular events participating to the fine-tuning of vWAT remodeling in obesity.

To shed light on the global molecular pattern associated to the different response of Low-INFL and Hi-INFL mice, we performed a proteomic analysis of their vWAT, which allowed the quantification of 6051 proteins. Among them, we found 175 and 510 differentially expressed proteins in Low-INFL and Hi-INFL, respectively, as compared to control vWATs (Figure 2A). Volcano plots in Figure 2B show the regulation profile of the 151 proteins commonly altered in both Low-INFL and Hi-INFL HFD groups. They include APOC2, APOC4, APOA4, LDLR, CIDEC, LPGAT1, AGPAT4, HMGCS1, whose function mainly relates to lipid metabolic processes, lipid transport, and endoplasmic reticulum stress (Figure 2C and Supplementary Tables 2-3). As expected, only the Hi-INFL vWAT proteome was enriched in proteins associated to inflammation (podosome regulation/activation, granulocyte and neutrophil activation, antigen receptor-mediated signaling pathway), such as MMP2, CASP1, CASP3, OPTN, ITGAM, ITGAD, LY9, PODXL, CD44, MCM7, GSTT1, reflecting the pro-inflammatory remodeling occurring within the tissue (Figure 2C). This observation confirms at global scale that inflammation is mainly occurring in vWAT of Hi-INFL mice, as opposed to Low-INFL. To

investigate which proteins and functions mainly differentiate the two HFD groups we performed supervised PLS-DA analysis (21). As shown in Supplementary Figure 1, while component 1 comprises the terms characterizing both Hi-INFL and Low-INFL compared to control, component 2, which accounts for about 6% of variability, includes the proteins discriminating Hi-INFL from Low-INFL vWATs. Of note, we found proteins involved in adipocyte function and marking adipocyte differentiation, such as adiponectin (ADIPOQ), hormone sensitive lipase (LIPE), fatty acid binding protein 4 (FABP4), resistin (RETN), and growth arrest-specific gene 6 (GAS6) as the five most discriminant variables of PLS-DA component 2 (Figure 2D, Supplementary Table 4). The expression profile of these proteins suggests that adipocyte differentiation is enhanced in Low-INFL compared to Hi-INFL, as further indicated by other proteins included in the dataset, such as the glucose transporter type 4 (SLC2A4), adipsin (CFD), beta-3 adrenergic receptor (ADRB3), perilipin 1 and 4 (PLIN1-4). Considering that all the mice used in this experiment shared the same genetic background and their genetic variability is very low, it is conceivable that epigenetic changes underlie the different behavior of Low-INFL and Hi-INFL groups. Therefore, we looked for chromatin modifier enzymes among the proteins that most differentiate Low-INFL from Hi-INFL vWAT, and we found four of them, including SET And MYND Domain Containing 3 (SMYD3), Elongator Acetyltransferase Complex Subunit 6 (ELP6), lysine (K)-specific demethylase 1A (KDM1A) and SWI/SNF related, matrix associated, actin dependent regulator of chromatin, subfamily d, member 2 (SMARCD2) (Figure 2B). Strikingly, GWAS studies have previously highlighted SNPs associated to phenotypes linked to inflammation(22) and/or obesity, such as BMI and waist to hip ratio in humans (23-26) for SMYD3, ELP6 and KDM1A. Furthermore, one of the hits, KDM1a (alias LSD1), whose expression is strongly reduced only in Hi-INFL mice, was already described as a repressor of adipocyte inflammatory gene (27), which further reinforce the potential interest of our dataset. Conversely, no information was available about the possible role of SMYD3, ELP6 and SMARCD2 in adipose tissue. We therefore checked their expression in two comprehensive datasets of all cell types populating vWAT (28, 29). Beyond KDM1, only SMYD3 was expressed in various adipose tissue cell types, including adipocytes, adipocyte progenitors and immune cells, in mouse, but also in human vWAT (Figure 2E and Supplementary figure 2). Conversely, ELP6 and SMARCD2 were almost not detected. We thus

focused our attention on SMYD3, a zinc binding protein with methyl-transferases activity, which gained attention in the last years as regulators of cell proliferation and developmental processes (30-32). SMYD3 protein expression pattern highlighted in vWAT by proteomic analysis was confirmed by western blot analysis (Figures 2F) and SMYD3 RNA levels showed a consistent expression pattern, although the changes did not reach statistical significance (Figure 2G).

We next explored the expression profile of SMYD3 in adipocytes by choosing a human *in vitro* model, namely adipose-derived human mesenchymal stem cells (AD-hMSCs) that can be differentiated into mature adipocytes(33)(Figure 3A). Interestingly, we found that SMYD3 is expressed in differentiating AD-hMSCs, and its mRNA and protein levels decrease rapidly along the differentiation process (Figure 3B-C), as opposed to known early and late differentiation markers, including CEBPB, CEBPA, PPARG (Figure 3D).

The high expression of SMYD3 in undifferentiated AD-hMSCs, together with its known regulatory function in cell cycle progression in other cell types, prompted us to explore whether SMYD3 plays a role in modulating cell proliferation also in our cellular model. We thus knocked down SMYD3 expression in proliferating AD-hMSCs 2 days before inducing adipocyte differentiation (day -2; Figure 4A). We significantly blunted SMYD3 levels at the induction of adipogenesis (day 0) and the reduction was still significant in cells differentiated for one day (Figure 4B). The consequences of SMYD3 silencing on cell growth were assessed by cell counting and MTT test. At day 0, no significant impact was observed on cell number and proliferation in undifferentiated AD-hMSCs (Figure 4C-D). In contrast, when we checked the effect of SMYD3 silencing 24h after the addition of the differentiation cocktail, we found that cell count and proliferation were significantly reduced in SMYD3 knocked-down AD-hMSCs (Figure 4C-D). This is very interesting in light of previous finding showing that several rounds of cell division occur also right after the induction of adipocyte differentiation *in vitro*, during the so-called mitotic clonal expansion (MCE), which is an important step for adipogenesis (34-36). Our results suggest that SMYD3 might be involved in the regulation of cell proliferation during the MCE occurring in AD-hMSCs at the very early stage of adipocyte differentiation. To further explore this possibility, we checked the effects of SMYD3 knock-down on

293 the expression of key regulators of MCE and adipogenesis, such as PPARγ, CEBPα and CEBPβ. No
294 effects were observed on PPARγ and CEBPα expression. In contrast, 24h following the induction of
295 the adipocyte differentiation, SMYD3 knock-down was accompanied by a significant reduction in the
296 levels of CEBPβ (Figure 4E-F), which is a key transcription factor necessary for the expansion of
297 early differentiating cells. Of note, the effect of SMYD3 knock-down on cell proliferation at the
298 beginning of adipocyte differentiation had also long-term consequences on lipid accumulation, as
299 demonstrated by the reduced Oil Red O staining in SMYD3 silenced cells, as compared to control
300 adipocytes (Figure 4G). Collectively, our results indicate SMYD3 as a new actor in the regulation of
301 adipocyte differentiation, in particular of the mitotic clonal expansion phase, possibly through
302 modulation of CEBPβ.

303

Discussion

Obesity is characterized by an increase of adipose tissue mass, which is generally associated to a high predisposition toward metabolic diseases, although some obese individuals seem protected toward the detrimental metabolic consequences of obesity. Recent GWAS studies have identified several independent loci whose genetic variance is associated to the susceptibility to obesity-driven metabolic perturbations(37, 38). Nevertheless, the genetic changes at population level cannot explain the rapid increment observed in the rate of obesity worldwide. Thus, a key role should exist for gene-environment interactions (39-41). In this context it is conceivable that epigenetic mechanisms, which are sensitive to environmental inputs, might contribute to regulate the individual vulnerability to obesity-driven detrimental consequences and research in this area is highly active. Our study arises from an observation obtained in a large group of C57Bl6 mice fed with a high fat diet for 8 weeks, of which about 20% had a significantly lower vWAT inflammation and systemic insulin resistance, despite a similar gain in adipose tissue mass. These mice, that we called Low-INFL, seemed thus protected against the development of obesity-driven inflammation and related metabolic consequences observed in the other mice fed with HFD (Hi-INFL), representing an invaluable experimental group to shed light on new key determinants of the susceptibility to obesity-driven detrimental effects.

Further large-scale investigations of vWAT proteomes of these mice confirmed the enrichment of proteins associated to the onset of an inflammatory response specifically in Hi-INFL HFD mice. Most interestingly, we found that many proteins involved in adipogenesis and/or adipocyte differentiation, including ADIPOQ, PLIN1, PLIN4, LIPE etc. were differentially expressed in Hi-INFL, as compared to Low-INFL vWAT. Our finding is consistent with previous reports suggesting that adipogenesis, by favoring a healthier expansion of adipose tissue, would prevent the obesity-mediated metabolic decline (8, 42). First, many genes associated with impaired expansion of adipose tissue are functionally associated with adipocytes/adipogenesis (37, 38, 43). In line with these observations, WAT depots from patients with metabolic syndrome are enriched in hypertrophic adipocytes and proinflammatory macrophages and present hypoxia and fibrosis (44, 45). Conversely, fat depots from metabolically healthy individuals contain a higher number of small adipocytes and have a relative high blood vessel

density (46). Several studies in mouse models also support the idea that the inability of WAT to adequately expand, to meet the energy storage demands, results in adipose tissue dysfunction. Pulse-chase genetic lineage tracing methods, which allow to track adipogenesis *in vivo*, have shown that a HFD rapidly triggers the commitment of adipocyte progenitors (APs), the first step necessary for adipogenesis (47). However, anti-adipogenic signals appear upon prolonged HFD feeding, thus impairing the terminal differentiation of adipocytes (16). Interestingly, such anti-adipogenic signals are activated preferentially in the visceral adipose tissue (vWAT) (16), which represents the fat depot more prone to develop obesity-related inflammation (48). Further suggesting the tight link between adipogenesis rate and the onset of inflammation in obese WAT, selective stimulation of *de novo* adipocyte differentiation in Pdgfrβ+ preadipocytes was shown to protect against pathologic visceral adipose expansion and inflammation (49).

Our finding that in Low-INFL mice adipogenesis is enhanced compared to Hi-INFL mice after 8 weeks of HFD raise questions about the regulators of adipocyte differentiation underlying such difference. Among the proteins showing a differential expression in Low-INFL and Hi-INFL vWAT, we found that KDM1a (alias LSD1) was significantly downregulated only in Hi-INFL mice. Such expression profile, together with the known role of KDM1 as a promoter of adipogenesis (15), is consistent with a dampened adipogenesis in Hi-INFL vWAT. In addition, we found that the histone methyltransferase SMYD3 was significantly induced only in Low-INFL vWAT. The family of SMYD methyl-transferases (SET and MYND domain-containing proteins) are well known regulators of cancer cell proliferation (30-32). More particularly, SMYD3 is frequently overexpressed in human cancers, and its high expression is associated with poor prognosis (50, 51). Recently, SMYD3 was also implicated in physiological developmental processes, such as myogenesis (52, 53) and iTreg differentiation (54, 55), while its role in adipose tissue is unknown. Of note, mice lacking SMYD3 are viable and often their phenotype appears only upon a given challenge (i.e. tumor induction), which suggests a role of this protein in the fine-tuning of specific tissue/cell responses that might alter susceptibility to disease. Consistent with this idea, a differential DNA methylation pattern at the SMYD3 gene was recently found in insulin sensitive obese women(56). Our results highlight for the first time SMYD3 as a new actor in

the regulation of adipocyte physiology. SMYD3 expression declines rapidly with differentiation, suggesting that its possible action should be played early in the process of adipogenesis. According to previous *in vivo* and *in vitro* findings, SMYD3 activity is critical in pathways regulating proliferation (31). Cell proliferating activity was observed at the very beginning (first 60 hours) of adipocyte differentiation, both in murine 3T3L1 and in AD-hMSCs (34-36, 57). This process, referred to as mitotic clonal expansion (MCE), results in three to four-fold increase of the total cell number thus modulating the number of cells capable of committing adipogenesis. Our data clearly indicate that SMYD3 might be involved in the regulation of cell proliferation at the early stages of adipogenesis induction, since its depletion at this moment reduces the number of cells, and, at longer term, reduces lipid accumulation in adipocytes. At the molecular levels, such effect is likely mediated by SMYD3 impact on the expression of CEBPβ, which is known to be required for MCE during adipogenesis (35)), whereas PPARγ and CEBPα are not affected. Future studies will be necessary to fully unravel SMYD3 function in adipose tissue and to understand how its activity can be modulated in physiology and disease.

Acknowledgements

This research was supported by Swiss National Science Foundation [grants #310030-156771) and #31003A-182420].

Author Contributions

TS performed proteomic analysis, data formal analysis and interpretation, data curation and visualization. **MG** performed *in vitro* experiments and data analysis and interpretation. **TC** performed *in vivo* experiments and data analysis. **NB** performed *in vivo* experiments. **MA** provided resources. **NW** and **AH** performed proteomics analysis and data processing. **TF** obtained funding. **AT** obtained funding and advised the study. **FG** conceived and supervised the study, analyzed and interpreted the data, obtained funding and wrote the manuscript. All authors have substantially contributed to the interpretation of the analyses, have revised the manuscript and have approved the final paper.

Competing Interests

The authors declare that they have no competing financial interests or personal relationships that could have appeared to influence the work reported in this paper

Data Availability Statement

The mass spectrometry proteomics data have been deposited to the ProteomeXchange Consortium via the PRIDE(58) partner repository with the dataset identifier PXD043165. All the other data generated during and/or analysed during the current study are available from the corresponding author on reasonable request.

Figure legends

Figure 1 Limited inflammatory response to HFD in low inflammation (Low-INFL) mice.

C57/BL6 male mice were fed for 8 weeks with control or HFD diet. Based on the onset of vWAT inflammation the mice fed with HFD were further divided in two groups. Low Inflammation (Low-INFL) mice had lower mRNA levels of markers of inflammatory cell infiltration (i.e. *chemokine (C-C motif) ligand 2 (Ccl2)*, Integrin Subunit Alpha X (*Itgax)*, and C-X-C motif chemokine ligand 12 (*Cxcl12*)) compared to high inflammation (Hi-INFL) mice (A) and lower levels of circulating insulin, leptin and resistin (B). The total mass of vWAT was similarly increased in Low-INFL and Hi-INFL mice (C). n=20 for control diet; n=19 for Low-INFL; n=34 for Hi-INFL. Bars represent mean ± SE. * P<0.05, ** P<0.01, *** P<0.001 versus control group; # P<0.05, ### P<0.001 vs Low-INFL group, as calculated by one-way ANOVA followed by Tukey's multiple comparisons test.

Figure 2 Proteomics analysis of vWAT of Low-INFL and Hi-INFL mice highlights SMYD3 as a possible player in their different response to the HFD.

(A) Venn diagram showing the number of proteins whose levels are significantly changed by HFD in Hi-INFL (orange circle) and Low-INFL (grey circle), as calculated by Limma (adj.p.<0.05, FC>1.5). n=6 (B) Volcano plots corresponding to the comparisons Hi-INFL versus control group (left) and Low-INFL versus control group (right). Differentially expressed proteins for the two comparisons (adj. p-value < 0.05) are colored in orange (common in both comparisons), dark red (comparison specific and overexpressed), or dark blue (comparison specific and underexpressed). (C) Biological pathways enriched within the differentially expressed proteins in Hi-INFL and Low-INFL with respect to control vWAT. (D) Fold changes of the expression of proteins involved in adipocyte function in Hi-INFL and Low-INFL as compared to control vWATs, * indicates significant changes versus control group; # indicates significant changes versus Low-INFL group, as calculated by Limma (adj.p.<0.05, FC>1.5). Values are represented as mean and are in logarithmic scale. (E) mRNA expression of SMYD3, KDM1A, ELP6 and SMARCD2 in the single cell atlas of mouse adipose tissue (29). ASPC: adipocyte stem and progenitor cell precursors; SMC: smooth muscle cells. LEC:lymphatic endothelial

cells. (F) Western Blot analysis of SMYD3 expression in control, Low-INFL and Hi-INFL vWAT and quantification of SMYD3 protein expression. (G) mRNA levels of SMYD3 in control, Low-INFL and Hi-INFL vWAT. Bars represent mean ± SE. # $P<0.05$ vs Hi-INFL group, as calculated by one-way ANOVA followed by Tukey's multiple comparisons test.

Figure 3 SMYD3 expression decreases along adipocyte differentiation

(A) Experimental scheme: confluent Adipose Derived hMSCs (AD-hMSCs) were differentiated to adipocytes with an adipogenic cocktail and samples were collected in undifferentiated cells (UnD) or 6h, 12h, 24h, 2days, 4 days, 7 days and 11 days after the induction of adipocyte differentiation. (B) mRNA and (C) protein levels of SMYD3. (D) mRNA levels of PPARG, CEBPA, and CEBPB in differentiating hMSCs. n=3. Bars represent mean ± SE. ** $P<0.01$; *** $P<0.001$ versus UnD samples, as calculated by one way ANOVA, followed by Dunnett's multiple comparison test.

Figure 4 SMYD3 regulates cell proliferation at the beginning of adipocyte differentiation

(A) Experimental scheme: siRNA of SMYD3 (siSMYD3) or with scrambled RNAs (CTRL) was performed in proliferating Adipose Derived hMSCs (AD-hMSCs). 2 days after cells differentiated to adipocytes. Cells were collected right before inducing differentiation (day 0), 24 hours after (day 1) or 14 days after adipogenesis induction. (B) SMYD3 RNA levels at day 0 and day 1. Cell number (n=6) and cell proliferation by MTT assay (n=6) were assessed at day 0 (C) and day 1 (D). PPARG, CEBPA and CEBPB mRNA levels were measured at day 0 (E) and day 1 (F) (n=3). Oil Red O staining was used to stain neutral lipids in cells differentiated for 14 days (G) (n=6). Representative pictures of cells transfected with siRNAs of SMYD3 (siSMYD3) or with scrambled RNAs (CTRL) are shown and the graph report Abs value of the extracted dye. Bars represent mean ± SE. ** $P<0.01$; *** $P<0.001$ versus CTRL samples, as calculated by student t-test.

References

1. Hruby A, Hu FB. The Epidemiology of Obesity: A Big Picture. Pharmacoeconomics. 2015;33(7):673-89.
2. Haczeyni F, Bell-Anderson KS, Farrell GC. Causes and mechanisms of adipocyte enlargement and adipose expansion. Obes Rev. 2018;19(3):406-20.
3. Gregor MF, Hotamisligil GkS. Inflammatory Mechanisms in Obesity. Annual Review of Immunology. 2011;29(1):415-45.
4. Appleton SL, Seaborn CJ, Visvanathan R, Hill CL, Gill TK, Taylor AW, et al. Diabetes and cardiovascular disease outcomes in the metabolically healthy obese phenotype: a cohort study. Diabetes Care. 2013;36(8):2388-94.
5. Hinnouho GM, Czernichow S, Dugravot A, Nabi H, Brunner EJ, Kivimaki M, et al. Metabolically healthy obesity and the risk of cardiovascular disease and type 2 diabetes: the Whitehall II cohort study. Eur Heart J. 2015;36(9):551-9.
6. Kim NH, Seo JA, Cho H, Seo JH, Yu JH, Yoo HJ, et al. Risk of the Development of Diabetes and Cardiovascular Disease in Metabolically Healthy Obese People: The Korean Genome and Epidemiology Study. Medicine (Baltimore). 2016;95(15):e3384.
7. Vishvanath L, Gupta RK. Contribution of adipogenesis to healthy adipose tissue expansion in obesity. J Clin Invest. 2019;129(10):4022-31.
8. Ghaben AL, Scherer PE. Adipogenesis and metabolic health. Nat Rev Mol Cell Biol. 2019;20(4):242-58.
9. Ling C, Ronn T. Epigenetics in Human Obesity and Type 2 Diabetes. Cell Metab. 2019;29(5):1028-44.
10. Emmett MJ, Lim HW, Jager J, Richter HJ, Adlanmerini M, Peed LC, et al. Histone deacetylase 3 prepares brown adipose tissue for acute thermogenic challenge. Nature. 2017;546(7659):544-8.
11. Ferrari A, Longo R, Fiorino E, Silva R, Mitro N, Cermenati G, et al. HDAC3 is a molecular brake of the metabolic switch supporting white adipose tissue browning. Nat Commun. 2017;8(1):93.
12. Ferrari A, Longo R, Peri C, Coppi L, Caruso D, Mai A, et al. Inhibition of class I HDACs imprints adipogenesis toward oxidative and brown-like phenotype. Biochim Biophys Acta Mol Cell Biol Lipids. 2020;1865(4):158594.
13. Wang L, Xu S, Lee JE, Baldridge A, Grullon S, Peng W, et al. Histone H3K9 methyltransferase G9a represses PPARgamma expression and adipogenesis. EMBO J. 2013;32(1):45-59.
14. Matsumura Y, Nakaki R, Inagaki T, Yoshida A, Kano Y, Kimura H, et al. H3K4/H3K9me3 Bivalent Chromatin Domains Targeted by Lineage-Specific DNA Methylation Pauses Adipocyte Differentiation. Mol Cell. 2015;60(4):584-96.

15. Musri MM, Carmona MC, Hanzu FA, Kaliman P, Gomis R, Parrizas M. Histone demethylase LSD1 regulates adipogenesis. J Biol Chem. 2010;285(39):30034-41.
16. Caputo T, Tran VDT, Bararpour N, Winkler C, Aguileta G, Trang KB, et al. Anti-adipogenic signals at the onset of obesity-related inflammation in white adipose tissue. Cell Mol Life Sci. 2021;78(1):227-47.
17. Amon S, Meier-Abt F, Gillet LC, Dimitrieva S, Theocharides APA, Manz MG, et al. Sensitive Quantitative Proteomics of Human Hematopoietic Stem and Progenitor Cells by Data-independent Acquisition Mass Spectrometry. Mol Cell Proteomics. 2019;18(7):1454-67.
18. Muntel J, Gandhi T, Verbeke L, Bernhardt OM, Treiber T, Bruderer R, et al. Surpassing 10 000 identified and quantified proteins in a single run by optimizing current LC-MS instrumentation and data analysis strategy. Mol Omics. 2019;15(5):348-60.
19. Ritchie ME, Phipson B, Wu D, Hu Y, Law CW, Shi W, et al. limma powers differential expression analyses for RNA-sequencing and microarray studies. Nucleic Acids Res. 2015;43(7):e47.
20. Yu G, Wang LG, Yan GR, He QY. DOSE: an R/Bioconductor package for disease ontology semantic and enrichment analysis. Bioinformatics. 2015;31(4):608-9.
21. Rohart F, Gautier B, Singh A, Le Cao KA. mixOmics: An R package for 'omics feature selection and multiple data integration. PLoS Comput Biol. 2017;13(11):e1005752.
22. Ahola-Olli AV, Wurtz P, Havulinna AS, Aalto K, Pitkanen N, Lehtimaki T, et al. Genome-wide Association Study Identifies 27 Loci Influencing Concentrations of Circulating Cytokines and Growth Factors. Am J Hum Genet. 2017;100(1):40-50.
23. Comuzzie AG, Cole SA, Laston SL, Voruganti VS, Haack K, Gibbs RA, et al. Novel genetic loci identified for the pathophysiology of childhood obesity in the Hispanic population. PLoS One. 2012;7(12):e51954.
24. Christakoudi S, Evangelou E, Riboli E, Tsilidis KK. GWAS of allometric body-shape indices in UK Biobank identifies loci suggesting associations with morphogenesis, organogenesis, adrenal cell renewal and cancer. Sci Rep. 2021;11(1):10688.
25. Zhu Z, Guo Y, Shi H, Liu CL, Panganiban RA, Chung W, et al. Shared genetic and experimental links between obesity-related traits and asthma subtypes in UK Biobank. J Allergy Clin Immunol. 2020;145(2):537-49.
26. Pulit SL, Stoneman C, Morris AP, Wood AR, Glastonbury CA, Tyrrell J, et al. Meta-analysis of genome-wide association studies for body fat distribution in 694 649 individuals of European ancestry. Hum Mol Genet. 2019;28(1):166-74.
27. Hanzu FA, Musri MM, Sanchez-Herrero A, Claret M, Esteban Y, Kaliman P, et al. Histone demethylase KDM1A represses inflammatory gene expression in preadipocytes. Obesity (Silver Spring). 2013;21(12):E616-25.

513 28. Sarvari AK, Van Hauwaert EL, Markussen LK, Gammelmark E, Marcher AB, Ebbesen MF, et
514 al. Plasticity of Epididymal Adipose Tissue in Response to Diet-Induced Obesity at Single-Nucleus
515 Resolution. Cell Metab. 2021;33(2):437-53 e5.
516 29. Emont MP, Jacobs C, Essene AL, Pant D, Tenen D, Colleluori G, et al. A single-cell atlas of
517 human and mouse white adipose tissue. Nature. 2022;603(7903):926-33.
518 30. Bernard BJ, Nigam N, Burkitt K, Saloura V. SMYD3: a regulator of epigenetic and signaling
519 pathways in cancer. Clin Epigenetics. 2021;13(1):45.
520 31. Bottino C, Peserico A, Simone C, Caretti G. SMYD3: An Oncogenic Driver Targeting
521 Epigenetic Regulation and Signaling Pathways. Cancers (Basel). 2020;12(1).
522 32. Shen H, Laird PW. Interplay between the cancer genome and epigenome. Cell.
523 2013;153(1):38-55.
524 33. Janderova L, McNeil M, Murrell AN, Mynatt RL, Smith SR. Human mesenchymal stem cells
525 as an in vitro model for human adipogenesis. Obes Res. 2003;11(1):65-74.
526 34. Tang QQ, Otto TC, Lane MD. Mitotic clonal expansion: a synchronous process required for
527 adipogenesis. Proc Natl Acad Sci U S A. 2003;100(1):44-9.
528 35. Tang QQ, Otto TC, Lane MD. CCAAT/enhancer-binding protein beta is required for mitotic
529 clonal expansion during adipogenesis. Proc Natl Acad Sci U S A. 2003;100(3):850-5.
530 36. Marquez MP, Alencastro F, Madrigal A, Jimenez JL, Blanco G, Gureghian A, et al. The Role
531 of Cellular Proliferation in Adipogenic Differentiation of Human Adipose Tissue-Derived
532 Mesenchymal Stem Cells. Stem Cells Dev. 2017;26(21):1578-95.
533 37. Chu AY, Deng X, Fisher VA, Drong A, Zhang Y, Feitosa MF, et al. Multiethnic genome-wide
534 meta-analysis of ectopic fat depots identifies loci associated with adipocyte development and
535 differentiation. Nat Genet. 2017;49(1):125-30.
536 38. Lotta LA, Gulati P, Day FR, Payne F, Ongen H, van de Bunt M, et al. Integrative genomic
537 analysis implicates limited peripheral adipose storage capacity in the pathogenesis of human insulin
538 resistance. Nat Genet. 2017;49(1):17-26.
539 39. Painter RC, Osmond C, Gluckman P, Hanson M, Phillips DI, Roseboom TJ. Transgenerational
540 effects of prenatal exposure to the Dutch famine on neonatal adiposity and health in later life. BJOG.
541 2008;115(10):1243-9.
542 40. Shi H, Su B. Molecular adaptation of modern human populations. Int J Evol Biol.
543 2010;2011:484769.
544 41. Stanner SA, Yudkin JS. Fetal programming and the Leningrad Siege study. Twin Res.
545 2001;4(5):287-92.
546 42. Nunn ER, Shinde AB, Zaganjor E. Weighing in on Adipogenesis. Frontiers in physiology.
547 2022;13:821278.

548 43. Justice AE, Karaderi T, Highland HM, Young KL, Graff M, Lu Y, et al. Protein-coding
549 variants implicate novel genes related to lipid homeostasis contributing to body-fat distribution. Nat
550 Genet. 2019;51(3):452-69.
551 44. Gustafson B, Hedjazifar S, Gogg S, Hammarstedt A, Smith U. Insulin resistance and impaired
552 adipogenesis. Trends Endocrinol Metab. 2015;26(4):193-200.
553 45. Kloting N, Bluher M. Adipocyte dysfunction, inflammation and metabolic syndrome. Rev
554 Endocr Metab Disord. 2014;15(4):277-87.
555 46. Carobbio S, Pellegrinelli V, Vidal-Puig A. Adipose Tissue Function and Expandability as
556 Determinants of Lipotoxicity and the Metabolic Syndrome. Adv Exp Med Biol. 2017;960:161-96.
557 47. Wang QA, Tao C, Gupta RK, Scherer PE. Tracking adipogenesis during white adipose tissue
558 development, expansion and regeneration. Nat Med. 2013;19(10):1338-44.
559 48. Strissel KJ, Stancheva Z, Miyoshi H, Perfield JW, 2nd, DeFuria J, Jick Z, et al. Adipocyte
560 death, adipose tissue remodeling, and obesity complications. Diabetes. 2007;56(12):2910-8.
561 49. Shao M, Vishvanath L, Busbuso NC, Hepler C, Shan B, Sharma AX, et al. De novo adipocyte
562 differentiation from Pdgfrbeta(+) preadipocytes protects against pathologic visceral adipose expansion
563 in obesity. Nat Commun. 2018;9(1):890.
564 50. Sarris ME, Moulos P, Haroniti A, Giakountis A, Talianidis I. Smyd3 Is a Transcriptional
565 Potentiator of Multiple Cancer-Promoting Genes and Required for Liver and Colon Cancer
566 Development. Cancer Cell. 2016;29(3):354-66.
567 51. Giakountis A, Moulos P, Sarris ME, Hatzis P, Talianidis I. Smyd3-associated regulatory
568 pathways in cancer. Semin Cancer Biol. 2017;42:70-80.
569 52. Codato R, Perichon M, Divol A, Fung E, Sotiropoulos A, Bigot A, et al. The SMYD3
570 methyltransferase promotes myogenesis by activating the myogenin regulatory network. Sci Rep.
571 2019;9(1):17298.
572 53. Fujii T, Tsunesumi S, Yamaguchi K, Watanabe S, Furukawa Y. Smyd3 is required for the
573 development of cardiac and skeletal muscle in zebrafish. PLoS One. 2011;6(8):e23491.
574 54. Nagata DE, Ting HA, Cavassani KA, Schaller MA, Mukherjee S, Ptaschinski C, et al.
575 Epigenetic control of Foxp3 by SMYD3 H3K4 histone methyltransferase controls iTreg development
576 and regulates pathogenic T-cell responses during pulmonary viral infection. Mucosal Immunol.
577 2015;8(5):1131-43.
578 55. Ting HA, de Almeida Nagata D, Rasky AJ, Malinczak CA, Maillard IP, Schaller MA, et al.
579 Notch ligand Delta-like 4 induces epigenetic regulation of Treg cell differentiation and function in
580 viral infection. Mucosal Immunol. 2018;11(5):1524-36.
581 56. Zhang SJ, Wang Y, Yang YL, Zheng H. Aberrant DNA Methylation Involved in Obese
582 Women with Systemic Insulin Resistance. Open Life Sci. 2018;13:201-7.

583 57. Qiu Z, Wei Y, Chen N, Jiang M, Wu J, Liao K. DNA synthesis and mitotic clonal expansion is
584 not a required step for 3T3-L1 preadipocyte differentiation into adipocytes. J Biol Chem.
585 2001;276(15):11988-95.
586 58. Perez-Riverol Y, Bai J, Bandla C, Garcia-Seisdedos D, Hewapathirana S, Kamatchinathan S,
587 et al. The PRIDE database resources in 2022: a hub for mass spectrometry-based proteomics
588 evidences. Nucleic Acids Res. 2022;50(D1):D543-D52.

589

Figures

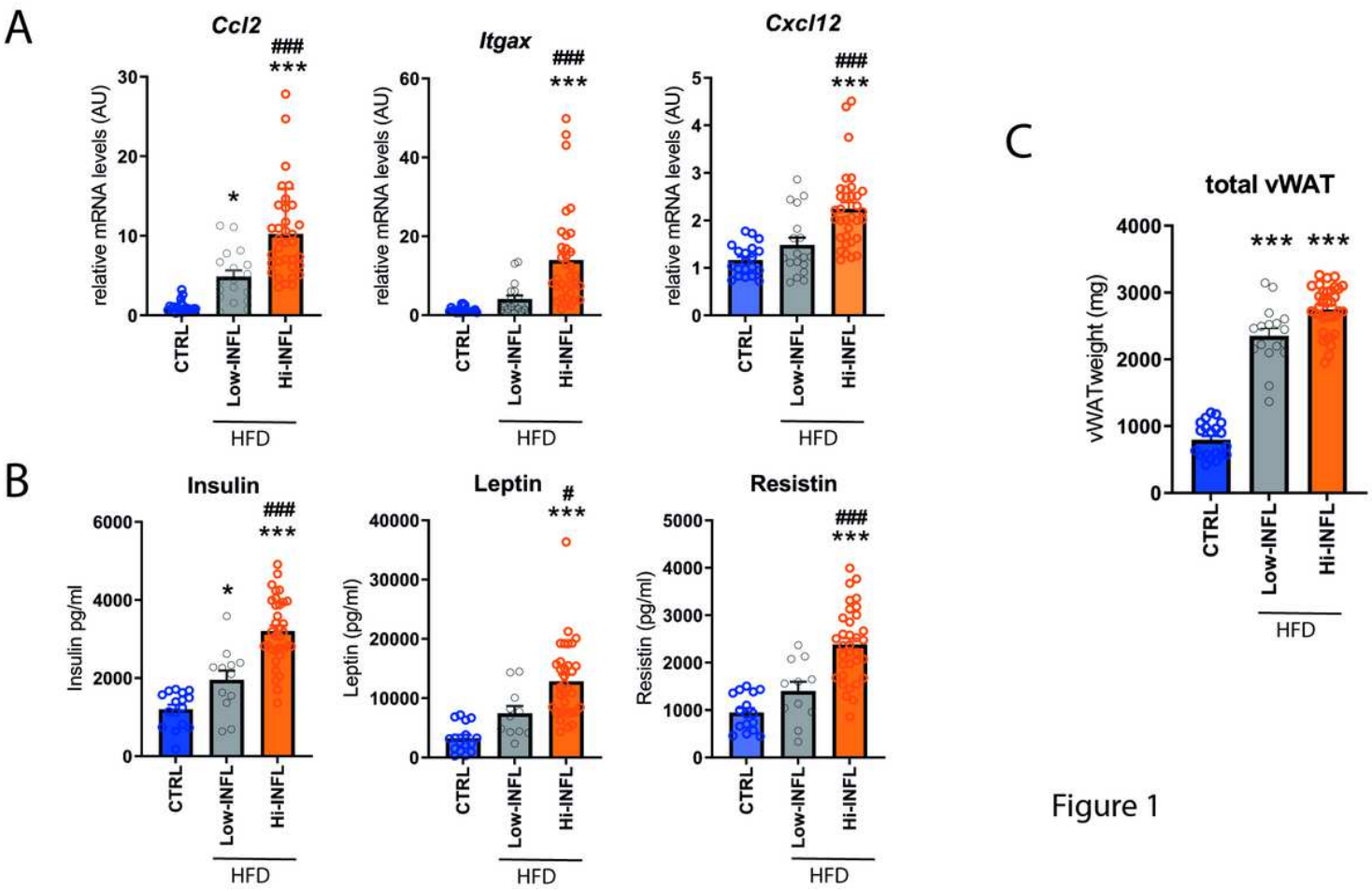

Figure 1

Limited inflammatory response to HFD in low inflammation (Low-INFL) mice.

C57/BL6 male mice were fed for 8 weeks with control or HFD diet. Based on the onset of vWAT inflammation the mice fed with HFD were further divided in two groups. Low Inflammation (Low- INFL) mice had lower mRNA levels of markers of inflammatory cell infiltration (i.e. chemokine (C-C motif) ligand 2 (Ccl2), Integrin Subunit Alpha X (Itgax), and C-X-C motif chemokine ligand 12 (Cxcl12)) compared to high inflammation (Hi-INFL) mice (A) and lower levels of circulating insulin, leptin and resistin (B). The total mass of vWAT was similarly increased in Low-INFL and Hi-INFL mice (C). n=20 for control diet; n=19 for Low-INFL; n=34 for Hi-INFL. Bars represent mean ± SE. * P<0.05, ** P<0.01, *** P<0.001 versus control group; # P<0.05, ### P<0.001 vs Low-INFL group, as calculated by one-way ANOVA followed by Tukey's multiple comparisons test.

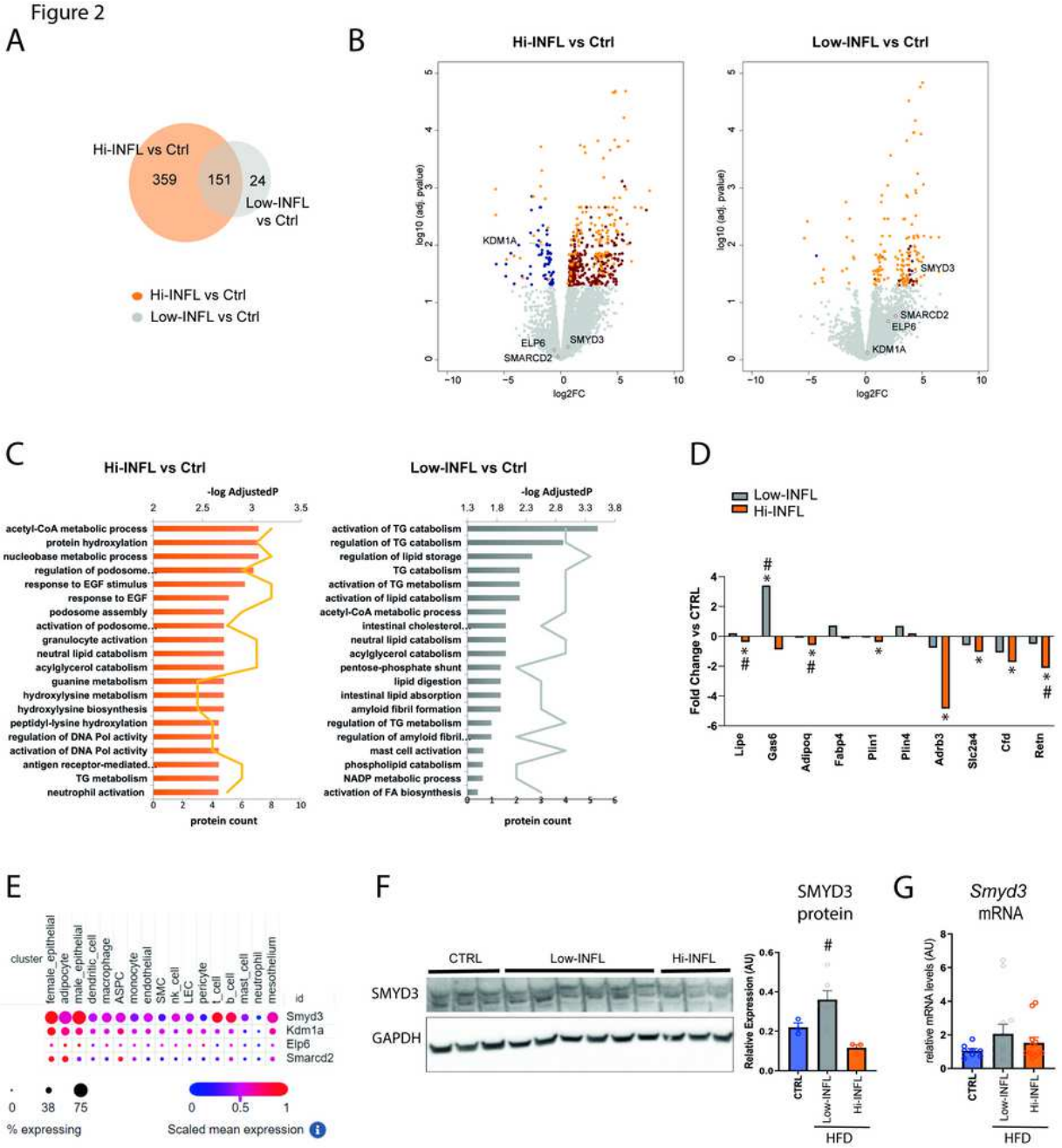

Figure 2

Proteomics analysis of vWAT of Low-INFL and Hi-INFL mice highlights SMYD3 as a possible player in their different response to the HFD.

(A) Venn diagram showing the number of proteins whose levels are significantly changed by HFD in Hi-INFL (orange circle) and Low-INFL (grey circle), as calculated by Limma (adj.p.<0.05, FC>1.5). n=6 (B)

Volcano plots corresponding to the comparisons Hi-INFL versus control group (left) and Low-INFL versus control group (right). Differentially expressed proteins for the two comparisons (adj. p-value < 0.05) are colored in orange (common in both comparisons), dark red (comparison specific and overexpressed), or dark blue (comparison specific and underexpressed). (C) Biological pathways enriched within the differentially expressed proteins in Hi-INFL and Low-INFL with respect to control vWAT. (D) Fold changes of the expression of proteins involved in adipocyte function in Hi- INFL and Low-INFL as compared to control vWATs, * indicates significant changes versus control group; # indicates significant changes versus Low-INFL group, as calculated by Limma (adj.p.<0.05, FC>1.5). Values are represented as mean and are in logarithmic scale. (E) mRNA expression of SMYD3, KDM1A, ELP6 and SMARCD2 in the single cell atlas of mouse adipose tissue (29). ASPC: adipocyte stem and progenitor cell precursors; SMC: smooth muscle cells. LEC:lymphatic endothelial cells. (F) Western Blot analysis of SMYD3 expression in control, Low-INFL and Hi-INFL vWAT and quantification of SMYD3 protein expression. (G) mRNA levels of SMYD3 in control, Low-INFL and Hi-INFL vWAT. Bars represent mean ± SE. # P<0.05 vs Hi-INFL group, as calculated by one-way ANOVA followed by Tukey's multiple comparisons test.

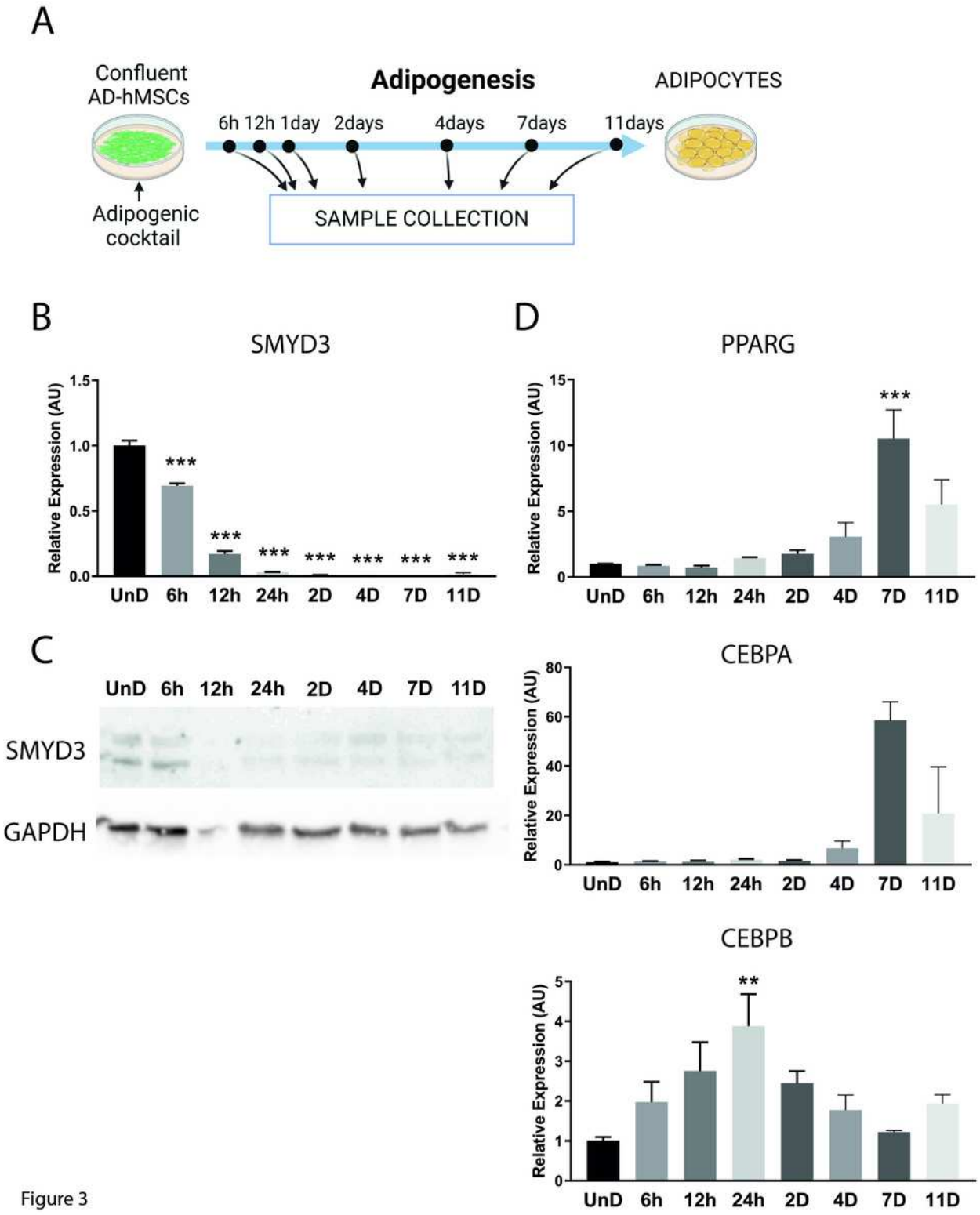

Figure 3

Figure 3

SMYD3 expression decreases along adipocyte differentiation

(A) Experimental scheme: confluent Adipose Derived hMSCs (AD-hMSCs) were differentiated to adipocytes with an adipogenic cocktail and samples were collected in undifferentiated cells (UnD) or 6h, 12h, 24h, 2days, 4 days, 7 days and 11 days after the induction of adipocyte differentiation. (B) mRNA

and (C) protein levels of SMYD3. (D) mRNA levels of PPARG, CEBPA, and CEBPB in differentiating hMSCs. n=3. Bars represent mean ± SE. ** P<0.01; *** P<0.001 versus UnD samples, as calculated by one way ANOVA, followed by Dunnett's multiple comparison test.

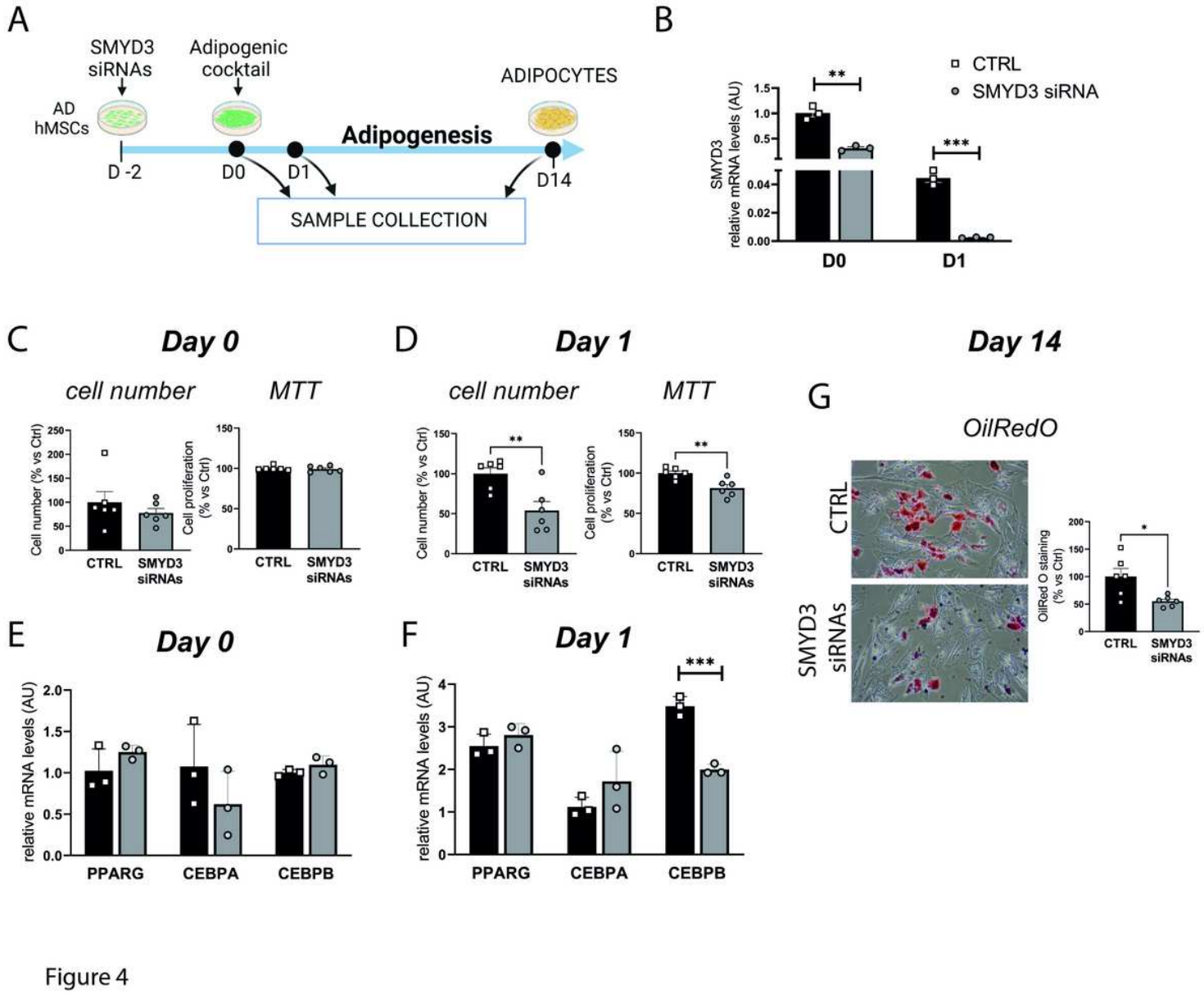

Figure 4

Figure 4

SMYD3 regulates cell proliferation at the beginning of adipocyte differentiation

(A) Experimental scheme: siRNA of SMYD3 (siSMYD3) or with scrambled RNAs (CTRL) was performed in proliferating Adipose Derived hMSCs (AD-hMSCs). 2 days after cells differentiated to adipocytes. Cells were collected right before inducing differentiation (day 0), 24 hours after (day 1) or 14 days after adipogenesis induction. (B) SMYD3 RNA levels at day 0 and day 1. Cell number (n=6) and cell

proliferation by MTT assay (n=6) were assessed at day 0 (C) and day 1 (D). PPARG, CEBPA and CEBPB mRNA levels were measured at day 0 (E) and day 1 (F) (n=3). Oil Red O staining was used to stain neutral lipids in cells differentiated for 14 days (G) (n=6). Representative pictures of cells transfected with siRNAs of SMYD3 (siSMYD3) or with scrambled RNAs (CTRL) are shown and the graph report Abs value of the extracted dye. Bars represent mean ± SE. ** P<0.01; *** P<0.001 versus CTRL samples, as calculated by student t-test.

Supplementary Files

This is a list of supplementary files associated with this preprint. Click to download.

- Sajicetal.Supplementalinformation.pdf
- Supplementarytable2.xlsx
- Supplementarytable3.xlsx
- Supplementarytable4.xlsx